Highest Mountains Suggest Strong Curvature of Shear Strength Envelopes for Rock

Mahendra Singh
Department of Civil Engineering, IIT Roorkee, Roorkee, INDIA

Nick Barton
NB&A, Oslo, Norway

ABSTRACT: The apparent 8 to 9km height limit of mountains will be addressed using critical state shear strength arguments, since confined compression strength is too high to explain these 'limited' heights. Modified Mohr Coulomb criteria have been derived based on critical state mechanics for rocks. These criteria are utilised to obtain estimates of maximum shear strength which actually is more likely to govern the height limit of mountains.

1 INTRODUCTION

There are fifteen mountains in the world with heights in the rarified range of 8 to 9km. The highest is Everest at approximately 8,848m. An extract from a Wikipedia photograph is shown in Figure 1. Since we are concerned with the ultimate strength of rock one can pose the question: why are the highest mountains no higher than 9km? Have mountains ever been higher than this during the earth's history? Since plate tectonics have been at work for a very long time, and contrary glacial processes also, one can perhaps assume that the extensive 'empirical evidence' that we see today is also a reflection of what has been in the recent and distant past. The strength of rock has little reason to have changed either, although it could be higher 'today' if the geothermal gradient had declined significantly.

In a well-known article written by Terzaghi (1962) near the end of his career: '*Stability of steep slopes on hard unweathered rock'*, a simple formulation of critical slope height was suggested: $H = q/\gamma$, where the uniaxial strength of rock and the vertical stress caused by its density are compared. The assumed vertical stress is estimated to be γH (or $\gamma H/100$ if using familiar MPa units as in rock mechanics). One can also use units kN/m^2 and kN/m^3 for the rock strength and density. Concerning the height of steep slopes, as opposed to mountains, Terzaghi suggested that the reason this formula over-predicted heights must be due to the presence of jointing. In fact, an explanation of cliff and mountain-wall heights has recently been developed as $H=\sigma_t/\gamma\nu$, involving the tensile strength of intact rock, density, and Poisson's ratio.

The even simpler 'Terzaghi' formula or its equivalent has been observed in use in internet 'chat sites' ('What rock strength is the highest mountain limited by?). The UCS/density formula (unfortunately) appears to produce a 'realistic' height for the highest mountains, when using the uniaxial strength of strong rocks such as 250MPa. However, at 9km depth, the rock mechanics reality concerning compression strength will be the 2 to 3 times higher polyaxially *confined* compression strength, and we do not accept 20-25km high mountains as being possible on earth, with our strong gravity. We need another explanation for the height 'limit' of apparently, about 9km.

Formation of high mountains due to colliding of plates in tectonically active region can be explained as shown in Fig. 2 (Nedoma, 1997). It was suggested that due to tectonic forces the lower plate bends downwards and releases horizontal tectonic stress. The horizontal stress becomes minor principal stress near the thrust. There is subsidence and normal faulting in the lower plate. The upper plate bends upwards and introduces compression and higher tectonic stress. The horizontal stress becomes major principal stress. This region experiences continuous uplifting in the form of mountains. The boundary of colliding plates experiences thrust faulting. The bottom part of the upper plate also bends upwards, due to which tangential stresses are released. Decrease in confining stress results in reduction of melting temperature of the rock and the rock melts. This molten rock may come out in the form of volcanoes.

Figure 1. Mount Everest, 8,864m (Wikipedia photo). Note that the peak of Everest is immediately behind the peak showing possible 'shear-planes'. (These cannot be tilted bedding). Misuse of the 'Terzaghi' formula: hc = 100 σ_c/γ gives an apparently correct answer for maximum mountain height (e.g.100 x 250/2.8 = 8.9km). The problem is that it has to be the confined strength of rock at 9 km depth, and this is much too high. Otherwise we would have 20-25km high mountains. Correct logic suggests a lower (critical state) shear strength limit, which may (also) be approximately 250 MPa. Figure 4 shows a possible explanation.

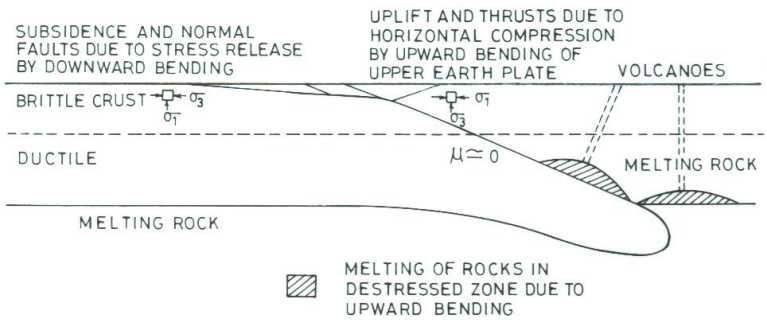

Figure 2. Precursors to the formation of high mountains due to interaction between colliding plate boundaries (Redrawn after Nedoma, 1997).

2 CONFINED COMPRESSIVE STRENGTH OF INTACT ROCKS

An appropriate failure criterion is required to obtain the confined compressive strength of intact rocks. The conventional linear Mohr-Coulomb criterion, though used extensively, has the limitation that the strength is assumed to be varying linearly with confining stress. It is a well accepted fact that variation in normal stress substantially alters the failure mode and the shear strength of the rock varies in a non-linear manner (Fig. 3) (Lockner and Beeler, 2002). For large variation in σ_n, like those occurring at great depths in the earth's crust, the non-linearity of the failure envelope substantially influences strength behaviour and should be considered while analysing strength behaviour.

In this context, the application of a critical state concept for rocks (Barton, 1976) has been found to be promising in correctly defining the strong curvature of the failure envelope (Singh and Singh, 2005; Singh et al., 2011, Shen et al. 2019). Barton (1976) postulated that *'the critical state for any intact rock is defined as the stress condition under which the Mohr-envelope of peak shear strength of the rocks reaches a point of zero gradient. This condition represents the maximum possible shear strength of the rock. For each rock, there will be a critical effective confining pressure above which the shear strength cannot be made to increase'*. With increasing

confining pressure, the failure mechanism passes through brittle, brittle-ductile-transition, ductile and finally critical state (Fig. 4). Barton's proposal for a critical state maximum possible shear strength was based on the observations of the strong curvature of the shear strength envelopes of numerous intact rocks, as demonstrated by Mogi (1966) (Fig. 4)

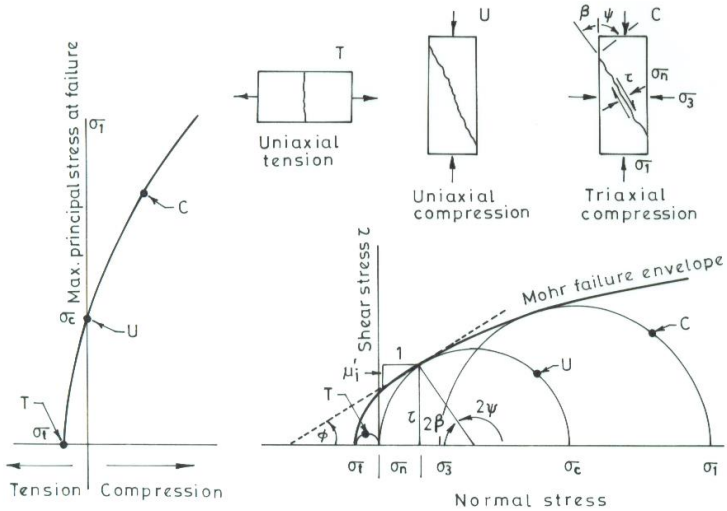

Figure 3. Mohr failure envelope showing relation between stresses and failure parameters (Redrawn from Lockner and Beeler, 2002)

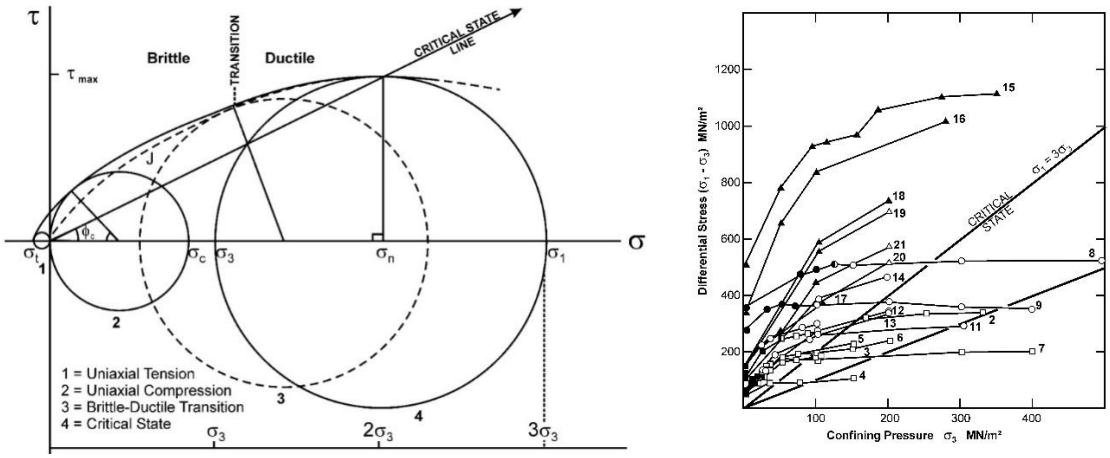

Figure 4. Observation of the strong curvature of the shear strength of intact rock at high confining pressure, with these examples from Mogi (1966) was the reason for proposing a critical state maximum possible shear strength in Barton (1976). Since this time a detailed study of more than 1,000 triaxial tests was performed by Singh et al. (2011), who verified that the majority of rocks exhibited close proximity, if not equality, of the UCS Mohr circle and the critical confining pressure needed to reach the critical stress (see σ_c and σ_3 sides of adjacent Mohr circles in the left-hand figure). Since σ_c is approximately numerically equal to τ_{max} due to the equality of the σ_c diameter and the radius of the critical Mohr circle, this simple 'geometry' can explain the high, but none the less limited shear strength of potential failure planes deep below the highest mountain chains.

The failure envelope for a well-known set of triaxial test data (Schwartz, 1964) reported in the literature (Hoek, 1983) is shown in Fig. 5. It is seen that the failure envelope approaches a point of zero gradient when confining stress is near 40 MPa. An evidence of a reduction in the friction angle is also given by Shankar et al. (2000). Based on back analysis, a friction angle of only 5° was reported for a depth of 40 km below the ground surface along the plate boundary in the Tibet Himalayan plate. It is interesting to note that the lesser the frictional resistance along colliding inter-plate boundaries, the lesser will be the locked-in strain energy in the large earth

plates. Therefore the chances of really great earthquakes in such an area are reduced. The largest earthquake that has taken place beneath the Tibetan plateau is ‘only’ M7 on Richter's scale (Singh et al., 2005).

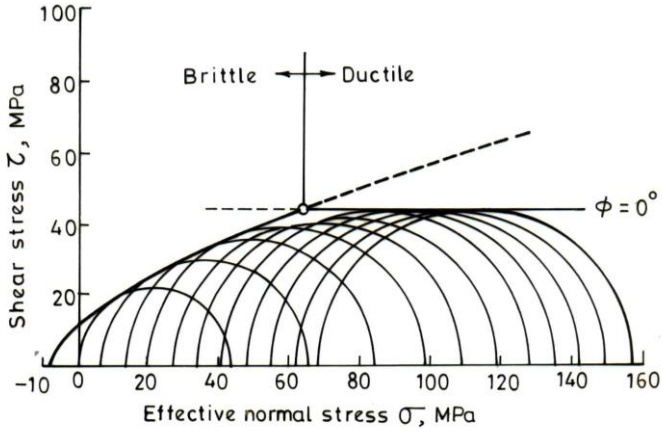

Figure 5. Critical state condition for Indiana limestone (Schwartz 1964; redrawn from Hoek, 1983).

2.1 *Critical State Concept Based Failure Criterion for Rocks*

By introducing a square term of confining pressure in the conventional linear Mohr-Coulomb failure criterion, Singh et al. (2011) suggested a Modified Mohr-Coulomb (MMC) criterion as follows:

$$(\sigma_1 - \sigma_3) = \sigma_{ci} + \frac{2\sin\phi_{i0}}{1-\sin\phi_{i0}}\sigma_3 - \frac{1}{\sigma_{crti}}\frac{\sin\phi_{i0}}{(1-\sin\phi_{i0})}\sigma_3^2 \quad \text{for } 0 \le \sigma_3 \le \sigma_{crti} \tag{1}$$

where

$$\sigma_{ci} = \text{UCS of the rock} = \frac{2c_{i0}\cos\phi_{i0}}{1-\sin\phi_{i0}} \tag{2}$$

Note: ϕ_{i0} = friction angle (MC parameter) of the rock for $\sigma_3 \to 0$, c_{i0}= cohesion (MC parameter) for the rock for $\sigma_3 \to 0$, σ_{crti} = critical confining pressure, the confining pressure at which the failure envelope in τ-σ space becomes horizontal. At $\sigma_3 = \sigma_{crti}$ the shear strength of rock will reach its maximum, the deviatoric stress at failure (σ_1-σ_3) will be constant for $\sigma_3 \ge \sigma_{crti}$.

$$(\sigma_1 - \sigma_3)_{max} = \sigma_{ci} + \frac{\sin\phi_{i0}}{1-\sin\phi_{i0}}\sigma_{crti} \qquad \text{for } \sigma_3 \ge \sigma_{crti} \tag{3}$$

The criterion has two parameters σ_{crti} and ϕ_{i0}. To get parameter σ_{crti}, Singh et al. (2011) back analysed a database comprising 154 triaxial data sets and came up with the suggestion that the critical confining pressure for an intact rock may be taken nearly equal to its UCS value. In the present study (2019) some additional data (from Shen et al., 2014; Jimenez, 2014) was added to the data base of Singh et al. (2011) to re-confirm the findings of Singh et al. (2011). The present data base comprises of the following extensive triaxial test data:

Table 1. The triaxial data sets available in the present analysis.

Rock type	No. of data sets	No. of triaxial tests
Igneous	42	293
Sedimentary	98	592
Metamorphic	63	371
Total	203	1256

The following steps were used to back analyse σ_{crti}:

i. Out of the two unknown parameters σ_{crti} and ϕ_{i0}, assume a first trial value of σ_{crti} as a multiple of UCS σ_{ci} (σ_{crti} = k.σ_{ci}). Say for example the first trial value is considered as 0.20 σ_{ci} (k=0.2),

ii. Consider the first triaxial test data set; the set includes UCS and a set of (σ_3, σ_1) values,

iii. Fit the failure criterion into the data and find out the best fitting value of the parameter ϕ_{i0} by least square method. Compute the percent error in prediction for each triaxial strength value as:

$$pe = abs\left(\frac{\sigma_{1cal} - \sigma_{1exp}}{\sigma_{1exp}} x100\right) \quad \text{percent} \tag{4}$$

where pe is the percent error in prediction, σ_{1exp} and σ_{1cal} are the experimental and the predicted values of triaxial strength of the rock.

iv. Compute the average percent error (avpe) for the particular data set as:

$$avpe = \sqrt{\frac{1}{npt}\sum_{i=1}^{npt}(pe^2)} \tag{5}$$

where npt is the number of data points in the data set.

v. Consider next data set and repeat steps iii and iv.

vi. In this way compute pe and avpe for all data sets and get overall average of the avpe value as:

$$\text{Overall average \% error} = \frac{\sum avpe}{\text{Number of data sets}} \tag{6}$$

vii Now consider the next trial value of σ_{crti} by assigning another value to the ratio k and repeat steps ii to vi. The computations are carried on until a very high k-value is reached.

Figure 6 shows the variation of overall average % error with the ratio $\sigma_{crti}/\sigma_{ci}$. The figure indicates that the overall average % error is minimum *when the critical confining pressure is taken nearly equal to the UCS of the intact rock.* A better insight can also be obtained by plotting the cumulative distribution function of the percent error in prediction, for individual data points. Figure 7 presents the cumulative distribution function of the percent error for various values of the ratio k. It can be seen that the minimum error is likely to occur in prediction when k is close to 1, i.e. the critical confining pressure is nearly equal to the UCS of the intact rock.

The failure criterion may therefore be written as:

$$(\sigma_1 - \sigma_3) = \sigma_{ci} + \frac{2\sin\phi_{i0}}{1 - \sin\phi_{i0}}\sigma_3 - \frac{1}{\sigma_{ci}}\frac{\sin\phi_{i0}}{(1 - \sin\phi_{i0})}\sigma_3^2 \quad \text{for } 0 \le \sigma_3 \le \sigma_{ci} \tag{7}$$

As per the critical state concept, the value of ϕ_i should approach zero as the rock enters the critical state. Beyond this, there will be no more increase in the frictional strength due to an increase in confining stress or normal stress. The shear strength will therefore reach a saturation limit as given below.

$$\tau_{max} = \frac{(\sigma_1 - \sigma_3)_{max}}{2} = \frac{\sigma_{ci}}{2(1 - \sin\phi_{i0})} \qquad \text{for } \sigma_3 \ge \sigma_{ci} \tag{8}$$

The UCS σ_{ci} is generally the most readily available property of intact rocks. The use of MMC criterion, therefore, needs only a single additional parameter ϕ_{i0} for its application. The parameter ϕ_{i0} represents the limiting value of the friction angle ϕ_i for $\sigma_3 \to 0$. Theoretically only a

single triaxial test is required (in addition to UCS) to get ϕ_{i0}. However, if more than one triaxial test data are available, the optimal value of the parameter ϕ_{i0} may be obtained as (Singh et el., 2011):

$$A_i = \frac{\sum(\sigma_1 - \sigma_3 - \sigma_{ci})}{\sum(\sigma_3^2 - 2\sigma_{ci}\sigma_3)}; \quad 0 < \sigma_3 \le \sigma_{ci} \tag{9}$$

$$B_i = -2A_i\sigma_{ci} \tag{10}$$

$$\sin\phi_{i0} = \frac{B_i}{2 + B_i} \tag{11}$$

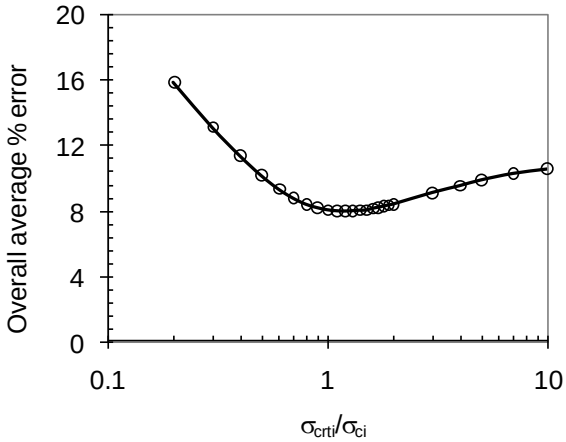

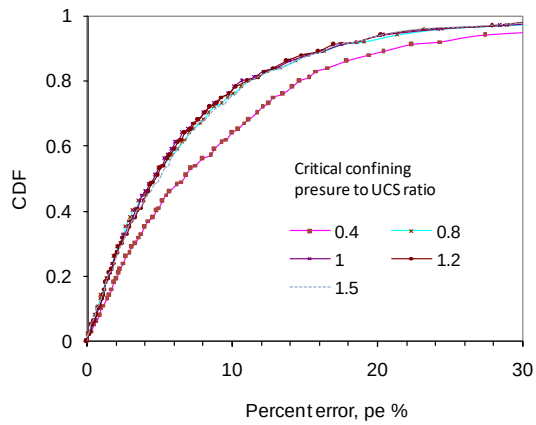

Left: Figure 6. Variation of overall average percent error with ratio $\sigma_{crti}/\sigma_{ci}$. Right: Figure 7. Cumulative distribution function of error in prediction of triaxial strength.

Alternatively, if triaxial test data are available for very low σ_3 values ($\sigma_3 \to 0$), it will be preferable to fit a linear criterion to determine c_{i0} and ϕ_{i0} by the least squares method and get σ_{ci} using Equation 2.

To demonstrate the applicability of the MMC, the triaxial test data of Indiana Limestone (Schwartz, 1964) has been considered. There are eleven data points including the UCS test (Table 2, Figure 5).

The Hoek-Brown parameters were computed by using all data points through the least squares method. For MMC, the critical confining pressure was taken equal to the UCS of the rock and the value of ϕ_{i0} was obtained through expressions given in Equations 9 to 11. The results are given in Table 2.

Table 2. Triaxial test data for Indiana limestone (Schwartz, 1964; source: Hoek, 1983)

σ_3 (MPa)	0	6.5	13.7	20.3	27.9	34.4	41.2	48.4	55.4	62.3	68.4
σ_1 (MPa)	44	66	85	99	109	119	128.2	135.1	141.9	149.1	156.5
HB Parameters: m=1.21, σ_{ci} = 60.66 MPa;											
MMC parameters: ϕ_{i0} = 30.7°; σ_{crti} = 44 MPa (UCS)											

The best fitting plots for the MMC and HB criteria are presented in Fig. 8. It is seen that the MMC fits better than the HB criterion. The MMC also reflects the strong curvature of the shear strength envelope.

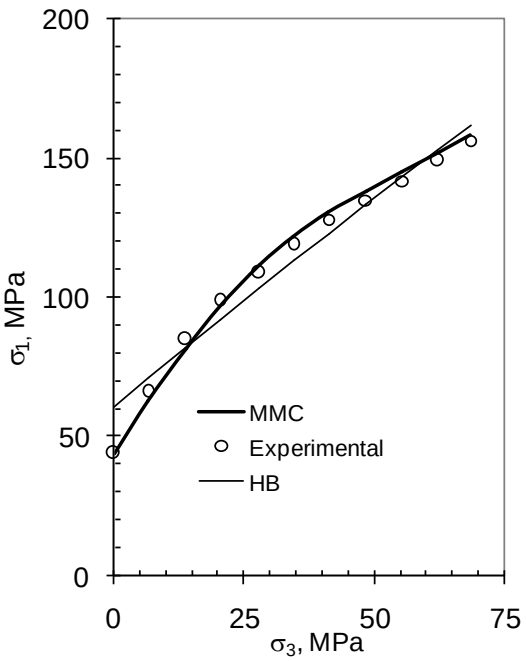

Figure 8. Best fitting plots for MMC and HB failure envelopes for Indiana Limestone

4 CONSEQUENCES OF STRONG CURVATURE OF THE SHEAR STRENGTH ENVELOPE

The consequences of the strong curvature of shear strength envelopes, actually stronger than that of the Hoek-Brown criterion for intact rock, have been further investigated by Shen et al. (2018), (2019), who demonstrated with the FRACOD fracture mechanics code (Shen et al. 2013) that a somewhat larger volume of rock would be fractured as a result of tunnel siting at 1 or 2km depth, as compared to the fracturing depth modelled with conventional models of shear strength. Shen managed to formulate relatively simple equations with recognisable input parameters, to describe both the tensile and compressive side of the non-linear shear strength, and more recently gave examples of typical strength envelopes (Shen et al. 2019) as illustrated in Figure 9. Approximate (numerical) conversion to the format σ_1 versus σ_3 shown in Figure 10, reinforces the impossibility of using the confined compressive strength of rock to estimate mountain height limits. The confined compression strength is just too high.

5 THE MAXIMMUM MOUNTAIN HEIGHT HYPOTHESIS

The critical state concept envisages that there is a maximum value up to which the shear strength of an initially intact rock may be made to increase due to confining pressure. As per the MMC this value is about equal to UCS for ϕ_{i0} equal to 30°, or slightly higher if ϕ_{i0} is more than 30°. The corresponding maximum σ_1 values will be of the order of 3 times UCS or more. Shen's recent formulations for the tensile and compressive regions of the strength envelope also re-confirm these findings. If the example of a rock with UCS of 250 MPa is considered (Fig. 10) it is estimated that the maximum principal stress will be on the order of three times the UCS i.e. more than about 750 MPa. If the corresponding maximum mountain height is obtained based on a maximum confined strength of 750 MPa and 27 kN/m^3 unit weight, it will come out to be 27.8 km. This computed height is of course much too large as compared to the actual maximum present height i.e. Everest's 8,848m.

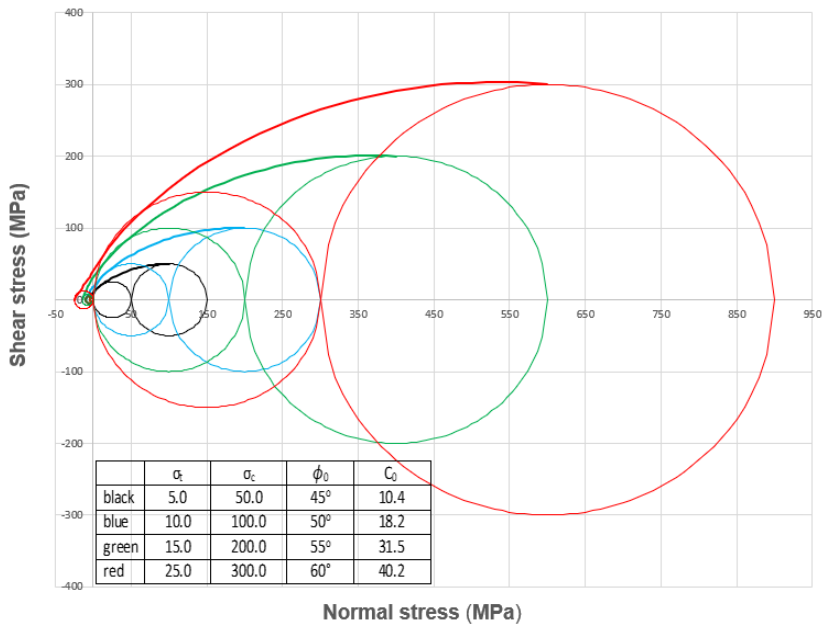

	σ_t	σ_c	ϕ_0	C_0
black	5.0	50.0	45°	10.4
blue	10.0	100.0	50°	18.2
green	15.0	200.0	55°	31.5
red	25.0	300.0	60°	40.2

Approximate nonlinear strength criteria with critical state for intact rocks.

Shen, Shi, Barton, 2019

$$\phi = \phi_0 - (45° - \phi_0)\frac{\sigma_n}{\sigma_t}$$

$$c = c_0 + (\sigma_t - c_0)\left(\frac{\sigma_n}{\sigma_t}\right)^2$$

$$\phi = \phi_0\left(1 - \sqrt{\frac{\sigma_n}{2\sigma_c}}\right)$$

$$c = c_0 + (\sigma_c - c_0)\frac{\sigma_n}{2\sigma_c}$$

Figure 9. Shen and Shi are responsible for the generation of the four example strength envelopes based on Shen's recent formulations for the tensile and compressive regions of the strength envelope shown on the right. The input data was suggested, so that the critical state theory of 1976 could be more easily understood as a logical and very simple strength criterion. Note the consequential touching Mohr circles for each set of input data (Shen et al. 2019).

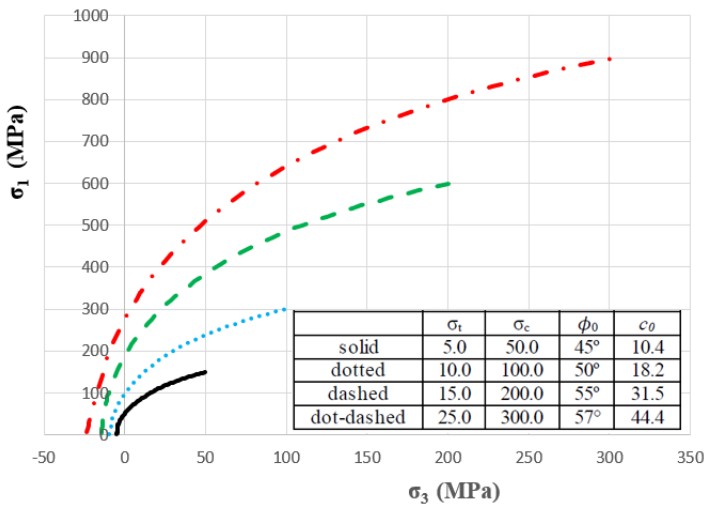

	σ_t	σ_c	ϕ_0	c_0
solid	5.0	50.0	45°	10.4
dotted	10.0	100.0	50°	18.2
dashed	15.0	200.0	55°	31.5
dot-dashed	25.0	300.0	57°	44.4

Figure 10. The confined compressive strength for rocks at e.g. 9km depth, where the confining pressure σ_3 might be of the order of 2.8 x 9,000/100 = 250 MPa, or perhaps higher due to the tectonic thrust against the Himalayas, where most of the highest peaks are found. This suggests that σ_1 will be much too high to explain 'only' 8 to 9km maximum mountain heights. Shen et al. 2019.

On the contrary, if the maximum height is obtained based on the maximum shear strength available, then for a UCS of 250 MPa, the maximum height will be about 250/27 = 9.25 km. This value roughly matches with the actual maximum heights in the Himalayas.

The suggested hypothesis is therefore that the maximum height of mountains is governed by the maximum shear strength available and not by the maximum compressive strength available.

6 CONCLUSIONS

By observing numerous strongly curved triaxial strength envelopes for silicates and carbonates presented by Mogi, 1966, who applied confining pressures in the range 100 to 500 MPa, the suggestion was made by Barton, 1976 that maximum strength (a horizontal strength envelope) would be reached along a line defined by the simple relation $\sigma_1 = 3\ \sigma_3$ critical. Some results presented in 1976 suggested that σ_3 critical was close to the value of UCS for the given rock. A hypothesis is suggested that the highest mountains of 8,000-9,000m are limited by maximum possible shear strength, not by maximum compressive strength. The critical state concept (Barton, 1976) was utilized to propose the Modified Mohr Coulomb (MMC) criterion to capture the strong curvature actually exhibited by rocks (Singh et al., 2011). Critical state mechanics has also been used recently to describe the tensile and compressive side of the non-linear shear strength (Shen et al. 2019). The maximum shear strength available has been found to be nearly equal to the UCS. It is observed that the maximum mountain height as computed from maximum available shear strength is very close to field values. There remain uncertainties concerning sub-Himalayan valley pore pressure levels, scale effects on UCS (therefore reducing maximum shear strength), and the absence or presence of highly stressed potential shear planes beneath the high mountains. Whether the rock is brittle or nearly ductile is another uncertainty. Potential shear planes beneath the highest mountains are presumably resisting the lateral loading due to plate tectonics, and the vertical loading due to the weight of overburden.

REFERENCES

Barton N. 1976. Rock Mechanics Review: The Shear Strength of Rock and Rock Joints, Int. J. Rock Mech. Min. Sci. & Geomech. Abstr., Vol.13, 255-279.

Hoek E. 1983. Strength of Jointed Rock Masses, Géotechnique, 23(3):187-223.

Jimenez R. 2014. Triaxial strength data for some rock types, Personal communication.

Lockner D.A. and Beeler N.M. 2002. Rock Failure and Earthquakes, International Handbook of Earthquake and Engineering Seismology, Eds. Lee, William H.K., Kanamori Hiroo, Jennings Paul C and Kisslinger Carl; Academic Press, Part A and B, Chapter-32, 505-537.

Mogi K. 1966. Pressure dependence of rock strength and transition from brittle to ductile flow. Bulletin of Earthquake Research Institution, 44: 215-32.

Nedoma J. 1997. Geodynamic Analysis of the Himalayas and the Andman Island, 29th General Assembly of IASPEI-97, Symposium S-3, Geodynamics of the Alpine Mediterranean Collision Zone, Greece.

Schwartz AE.1964. Failure of Rock in the Triaxial Shear Test, Proc.,6th Symp. Rock Mechanics, Rolla, Mo.,1964, 109–135.

Shankar D., Kapur, N. and Singh, B. 2000. Thrust-Wedge Mechanics and Coeral Development of Normal and Reverse Wedge Faults in the Himalayas, J. Geological Society, London, Vol 159, 273-280.

Shen J, Jimenez R, Karakus M, Xu c. 2014. A Simplified Failure Criterion for Intact Rocks Based on Rock Type and Uniaxial Compressive Strength, Jl. Rock Mech. Rock Engineering., 47(2), 357-369.

Shen B., Shi J. and Barton N. 2018. An Approximate Non-Linear Modified Mohr-Coulomb Shear Strength Criterion with Critical State for Intact Rocks. Journal of Rock Mech. & Geotech. Eng. 645-652.

Shen B., Shi J. and Barton N. 2019. Graphic examples of a logical non-linear strength criterion for intact rock. Rock Mechanics and Rock Engineering. In press.

Singh M. and Singh B. 2005. A Strength Criterion Based on Critical State Mechanics for Intact Rocks, Rock Mech & Rock Engineering, 38 (3), July-Sept 2005, 243–248.

Singh M. Raj A. Singh B. 2011. Modified Mohr-Coulomb Criterion for Non-linear Triaxial and Polyaxial Strength of Intact Rocks, Int J Rock Mech Mining Sci, 48(4), 546-555.

Singh M., Singh B. and Shankar D. 2005. Critical State Mechanics in Non-Linear Failure Criterion for Rocks, Journal of Rock Mechanics and Tunnelling Technology, 11(1), 13-24.

Terzaghi K. 1962. Stability of Steep Slopes on Hard Unweathered Rock, Géotechnique, 12(4):251-270.